Numerical Study on a Sliding Bubble During Nucleate Boiling

Gihun Son*
Department of Mechanical Engineering, Sogang University, Seoul 121-742, Korea

A numerical method for simulating bubble motion during nucleate boiling is presented. The vapor-liquid interface is captured by a level set method which can easily handle breaking and merging of the interface and can calculate an interfacial curvature more accurately than the VOF method using a step function. The level set method is modified to include the effects of phase change at the interface and contact angle at the wall as well as to achieve mass conservation during the whole calculation procedure. Also, a simplified model to predict the heat flux in a thin liquid microlayer is developed. The method is applied for simulation of a sliding bubble on a vertical surface to further understand the physics of partial nucleate boiling. Based on the computed results, the effects of contact angle, wall superheat and phase change on a sliding bubble are quantified.

Key Words : Level Set Method, Sliding Bubble, Nucleate Boiling, Contact Angle

Nomenclature

c_p : Specific heat at constant pressure
g : Gravity
H : Step function
h : Grid spacing
h_{ev} : Evaporative heat transfer coefficient
h_{fg} : Latent heat of evaporation
k : Thermal conductivity
L : Length scale,
Nu : Nusselt number,
$\vec{n}$: Normal unit vector
p : Pressure
q : Heat flux
R : Effective radius of a bubble
R_{gas} : Gas constant
$R_{\min}$: Minimum bubble radius for sliding
T : Temperature
ΔT : $T_w - T_{sat}$
U : Bubble slide velocity
u, v : x, y-directional velocities
$\vec{u}$: Velocity vector, (u, v)
$\dot{V}_{micro}$: Rate of vapor volume production from the microlayer
ΔV_{micro} : Control volume surrounding the liquid microlayer
x, y : Horizontal and vertical coordinates

Greek Symbols

δ : Liquid film thickness
κ : Interfacial curvature
μ : Dynamic viscosity
ρ : Density
σ : Surface tension
τ : Artificial time
ϕ : Level set function
φ : Contact angle

Subscripts

1, 2 : Points 1 and 2
A, R : Advancing, receding
int : Interface
l, v : Liquid, vapor
sat, w : Saturation, wall

* **E-mail** : gihun@ccs.sogang.ac.kr
TEL : +82-2-705-8641 ; **FAX** : +82-2-712-0799
Department of Mechanical Engineering, Sogang University, Seoul 121-742, Korea. (Manuscript **Received** October 30, 2000; **Revised** April 10, 2001)

1. Introduction

Despite extensive studies of nucleate boiling, bubble growth and detachment observed during

nucleate boiling is not yet understood well. This is caused by the fact that most of the previous studies have overly simplified bubble dynamics and have not correctly analyzed the flow and temperature fields influenced by the bubble motion.

Van Helden et al. (1995) observed the departure of a bubble sliding on a vertical surface and derived expressions for the forces on a detaching bubble. Although the coefficients for each force were quantified from the data measured experimentally, the detachment diameter could not be obtained by just balancing the forces acting on the bubble because the sum of these forces should be zero at all times. Thorncroft et al. (1998) also performed visual experiments to investigate the mechanism of the bubble growth and detachment. However, they could not identify the force responsible for vapor bubble detachment during vertical pool boiling.

As one approach to further clarify such bubble dynamics associated with partial nucleate boiling, direct numerical simulation of a growing and departing bubble has been made recently. Lee and Nydahl (1989) simulated the bubble growth on a horizontal surface using a coordinate transformation technique supplemented by a numerical grid generation method. Although Lee and Nydahl solved numerically the momentum and energy equations, they had to assume that the bubble remained hemispherical in shape during its growth. To obtain the bubble shape as part of the solutions, Welch (1998) carried out more generalized computations of vapor bubble growth. However, his method was not extended to flows with large interfacial distortion. Takata et al. (1998) simulated a helium bubble growing and departing on a heated surface incorporating the effect of phase change in a VOF(Volume of Fluid) method, where the interface is implicitly captured by the step function representing the volume fraction in each cell. Thus, this method could handle the bubble departure process. However, their computations could not be made for test fluid with large liquid-vapor density ratio.

To calculate incompressible two-phase flows with large density ratios, Sussman et al. (1994) developed a level set method where the level set function is defined as a signed distance from the interface. Since the distance function and its spatial derivatives are smooth and continuous, the level set method can be used to compute an interfacial curvature more accurately than the VOF method using a step function. However, the discretization of the level set formulation is found not to preserve total mass conservation. Son et al. (1999) modified the level set formulation to accommodate a phase change effect and performed numerical simulation of a water bubble growing and departing on a horizontal surface. Also, the effect of microlayer evaporation was included in the analysis.

In this study, a sliding bubble on a vertical heated surface is numerically computed to further clarify its behavior which was not well explained from the previous experimental studies. The level set method modified to include the effect of phase change is improved to achieve mass conservation during the whole calculation procedure. Also, a simplified model to predict the heat flux in a thin liquid microlayer is developed to efficiently simulate a sliding bubble with contact angles changing.

2. Numerical Formulation

Figure 1 shows the configuration used in this study to simulate a sliding bubble on a vertical surface. The bubble attached to the surface forms

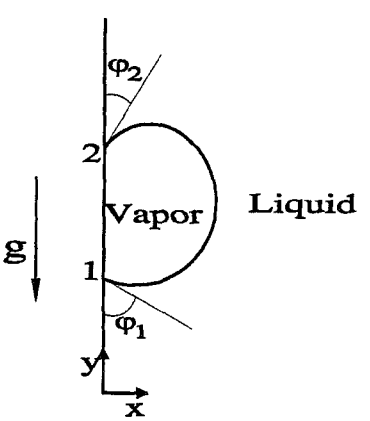

Fig. 1 Configuration of a sliding bubble on a vertical surface

two contact lines at points 1 and 2. Computations are performed for two-dimensional flow associated with a cylindrical bubble sliding on a vertical surface, which is different from a spherical type of bubble observed during nucleate boiling. The spherical type of bubble can be obtained only through fully three-dimensional computation, which is one of the most challenging numerical problem still remaining to be solved. In this first study on a sliding bubble during nucleate boiling, we have employed two-dimensional approach which is simple but can describe qualitatively key features of a sliding bubble on a vertical surface. It is assumed that the flows are laminar and the fluid properties including density, viscosity and thermal conductivity are constant in each phase.

2.1 Governing equations

The interface separating the two phases is captured by ϕ which is defined as a signed distance from the interface. The negative sign is chosen for the vapor phase and the positive sign for the liquid phase. In carrying out numerical simulation, the computational domain is moved with the slide velocity of a bubble to prevent the bubble from escaping out of the computational domain. The mass, momentum and energy equations for the vapor-liquid region can be written as (Son et al., 1999)

$$\begin{aligned}
&\nabla\cdot\vec{u}=\frac{(\vec{u}_{\text{Int}}-\vec{u})}{\rho}\cdot\nabla\rho+\dot{V}_{micro}\\
&\rho\frac{D\vec{u}}{Dt}=-\nabla p+\rho\vec{g}-\sigma\kappa\nabla H\\
&\qquad\qquad +\nabla\cdot\mu[\nabla\vec{u}+(\nabla\vec{u})^T] \qquad (1)\\
&\rho_{Cp}\frac{DT}{Dt}=\nabla\cdot k\nabla T \quad for \quad H>0\\
&T=T_{sat} \qquad\qquad for \quad H=0
\end{aligned}$$

where

$$\begin{aligned}
&\vec{u}_{int}=\vec{u}+k\nabla T/\rho h_{fg}\\
&\frac{D}{Dt}=\frac{\partial}{\partial t}+(\vec{u}+U\vec{g}/g)\cdot\nabla\\
&\rho=\rho_v(1-H)+\rho_l H;\ \mu^{-1}=\mu_v^{-1}(1-H)+\mu_l^{-1}H\\
&\rho_{Cp}=\rho_l C_{pl}H;\qquad k^{-1}=k_l^{-1}H\\
&H=1 \qquad\qquad if\ \phi\geq 1.5h\\
&\ =0 \qquad\qquad if\ \phi\leq -1.5h\\
&\ =\frac{1}{2}+\frac{\phi}{3h}+\frac{\sin(2\pi\phi/3h)}{2\pi} \qquad if\ |\phi|<1.5h
\end{aligned}$$

Here, U is the slide velocity of a bubble and h is a grid spacing. In the mass conservation equation, $\dot{V}_{micro}$ is the vapor production rate from the microlayer which is defined as a liquid layer near the locations the bubble contacts the wall as marked by points 1 and 2 in Fig. 1. The microlayer has a thickness varying from the nonevaporating film thickness to $h/2$, which is the distance to the first computational node for from the wall. Then, $\dot{V}_{micro}$ is obtained as

$$\dot{V}_{micro}=\int\frac{k_l(T_W-T_{int})}{\rho_v h_{fg}\delta\Delta V_{micro}}\,dy_{micro} \qquad (2)$$

where δ is the microlayer thickness and ΔV_{micro} is a control volume surrounding the microlayer. In Eq. (2), the interface temperature, T_{int}, has to rise up to the wall temperature as the thickness of the liquid microlayer decreases; otherwise there would be a singularity where the bubble contacts the wall. This can be avoided by using a lubrication formulation.

2.2 Liquid microlayer formulation

The governing equations for the liquid microlayer can be obtained using a lubrication theory (Wayner, 1992; Lay and Dhir, 1995; Son et al., 1999). In this study, however, a simplified model for the microlayer is developed to efficiently compute a sliding bubble with contact angles changing. Using the energy conservation for the liquid microlayer and a modified Clausis-Clayperon equation (Wayner, 1992), the heat flux from the microlayer is written as

$$q=k_l\frac{(T_W-T_{int})}{\delta}=h_{ev}\Big[T_{int}-T_{sat}+(P_l-P_v)\frac{T_{sat}}{\rho_l h_{fg}}\Big] \qquad (3)$$

where

$$h_{ev}=\sqrt{\frac{2}{\pi R_{gas}T_{sat}}}\,\frac{\rho_v h_{fg}^2}{T_{sat}}$$

Assuming the pressure jump at the liquid-vapor interface, p_l-p_v, does not contribute significantly for the heat flux from the microlayer, Eq. (3) is simplified as

$$q=(T_W-T_{sat})/\Big(\frac{\delta}{k_l}+\frac{1}{h_{ev}}\Big) \qquad (4)$$

It is noted from the results for the liquid microlayer obtained by Son et al. (1999) that the interface in the microlayer has a nearly constant slope except near the nonevaporating region where the slope decreases to zero rapidly. Thus, the interface slope in the microlayer is assumed to be constant as

$$\frac{d\delta}{dy}=\tan\varphi \tag{5}$$

where φ is an apparent contact angle. Substitution of Eq. (4) and Eq. (5) into Eq. (2) yields

$$\dot{V}_{micro}=\frac{k_l(T_w-T_{sat})}{\rho_v h_{fg}\Delta V_{micro}}\frac{1}{\tan\varphi}\ln\left(\frac{h}{2}\frac{h_{ev}}{k_l}+1\right) \tag{6}$$

The total vapor production rate through the microlayer obtained from Eq. (6) is found to be in good agreement with that obtained from the microlayer analysis of Son et al. (1999). The error is less than 1 percent as long as h is not reduced up to k_l/h_{ev}. This kind of simplified model for the microlayer was also reported by Khrustalev and Faghri (1995).

2.3 Level set formulation

In the level set formulation, the level set function is advanced and reinitialized as

$$\frac{D\phi}{Dt}=-(\vec{u}_{\text{int}}-\vec{u})\cdot\nabla\phi \tag{7}$$

$$\frac{\partial\phi}{\partial\tau}=\frac{\phi_o}{\sqrt{\phi_o^2+h^2}}(1-|\nabla\phi|) \tag{8}$$

where ϕ_o is a solution of Eq. (7) and τ is an artificial time. While the level set formulations given by Eqs. (7) and (8) are computed numerically, it is found that the total mass of vapor-liquid region is not conserved well. To remove such a volume loss problem and to preserve total mass conservation during the whole calculation procedure, the following volume correction step is added to the level set formulation:

$$\frac{\partial\phi}{\partial\tau}=(V-V_o)|\nabla\phi| \tag{9}$$

where V is a bubble volume computed from ϕ and V_o is the bubble volume when satisfying mass conservation.

2.4 Boundary conditions

The boundary conditions used in this study are as follows:

at the wall,

$$\vec{u}=0,\ T=T_w,\ \vec{n}\cdot\nabla\phi=-\cos\varphi \tag{10}$$

at the slip boundaries (the right side and the bottom of the domain),

$$\vec{n}\cdot\vec{u}=0,\ \vec{n}\cdot\nabla\vec{u}\times\vec{n}=0,\ \vec{n}\cdot\nabla T=\vec{n}\cdot\nabla\phi=0 \tag{11}$$

at the top of the domain,

$$\vec{n}\cdot\nabla\vec{u}=0,\ \vec{n}\cdot\nabla T=\vec{n}\cdot\nabla\phi=0 \tag{12}$$

In Eq. (10), the contact angle used as a wall boundary condition for a level set depends on the nature of a solid surface. For an ideal surface without contact angle hysteresis, the contact angle has a single value. However, for real surfaces heterogeneous and rough, the contact angle varies dynamically between an advancing (or maximum) contact angle, φ_A, and a receding (or minimum) contact angle, φ_R, which is expressed as $\varphi_R\leq\varphi_1$, $\varphi_2\leq\varphi_A$. As long as the contact angle changes in the range of $\varphi_R<\varphi<\varphi_A$, the location the bubble contact the wall does not move, which corresponds to a "stick" stage called by Marmur (1998). However, while the contact line moves, which corresponds to a "slip" stage, the contact angle remains constant as $\varphi=\varphi_R$ or $\varphi=\varphi_A$ depending on the moving direction of the contact line.

3. Results and Discussion

In carrying out numerical simulation, the length scale and the velocity scale are defined as $L=\sqrt{\sigma/g(\rho_l-\rho_v)}$ and $\sqrt{gL}$, respectively. Also, the physical parameters necessary for computations are evaluated from the properties of saturated water at one atmosphere pressure. Using the properties, L is evaluated as 2.5 mm.

First, the level set formulation was tested for its accuracy by comparing the predicted terminal velocities of bubbles rising in a stationary liquid with the results obtained by Ryskin and Leal (1984) using a body-fitted grid (Son and Lee, 1999). The difference between both results was less than 3 percent. Also, the numerical solutions

of an unsteady one-dimensional problem with phase change showed good agreement with the analytical solutions.

3.1 A sliding bubble without phase change

Results are first presented for sliding bubbles without phase change. The computations were performed using mesh points of 66×194 and the computational domain of $2L\times6L$.

The sliding condition of a bubble attached to a vertical surface is determined by the bubble size and the contact angles. By balancing the buoyancy with the surface tension force acting on a static bubble shown in Fig. 1 and setting $\varphi_2=\varphi_R$ and $\varphi_1=\varphi_A$, the minimum bubble radius required for sliding is obtained as

$$R_{min}/L=\sqrt{(\cos\varphi_R-\cos\varphi_A)/\pi} \qquad (13)$$

It is noted from Eq. (13) that for an ideal surface with $\varphi_A=\varphi_R$, bubbles of all sizes slide along the vertical surface. For a non-ideal surface with φ_A and φ_R different, bubbles smaller than R_{min} remain stationary on the surface. To illustrate such phenomena, computations are made using the parameters of $R=0.7075$ mm, $\varphi_R=45°$ and two different advancing contact angles, $\varphi_A=90°$ and $\varphi_A=70°$.

According to Eq. (13), R_{min} is 1.175 mm for $\varphi_R=45°$ and $\varphi_A=90°$. When φ_A is reduced up to 70°, R_{min} becomes 0.85 mm. Thus, the bubble with a radius of 0.7075 mm is expected not to slide along the vertical surface. The results obtained from the numerical simulations are plotted in Fig. 2. The initial shape of a bubble is taken to be a circular arc with $\varphi_1=\varphi_2=\varphi_A$. It is seen from Fig. 2 (a) that during the early period of the computations, the slide velocity of a bubble is oscillating due to unbalance between the buoyancy and surface tension forces. However, as the bubble shape is deformed so that the surface tension force is balanced with the buoyancy, the oscillation decays with time and then the bubble becomes stationary on the surface. Figure 2 (b) shows the bubble shapes at the stationary state where the contact angles at points 1 and 2 are obtained for two cases as:

$$\varphi_R=45°<\varphi_1=84°,\ \varphi_2=69°<\varphi_A=90°$$

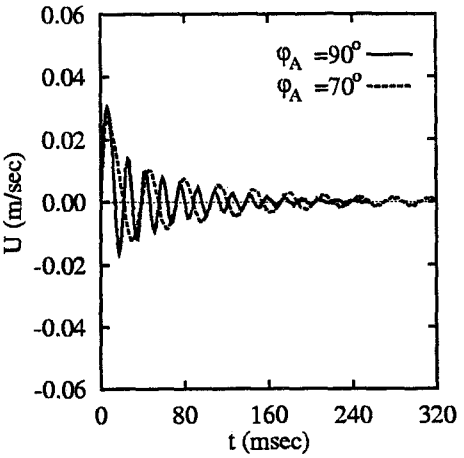

(a)

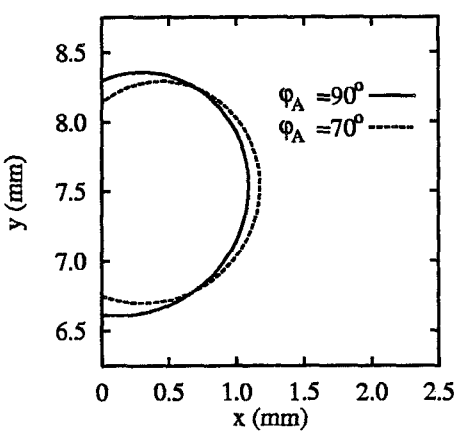

(b)

Fig. 2 Stationary bubbles: (a) bubble slide velocity and (b) bubble shape at a steady state for $R=0.7075$ mm, $\varphi_R=45°$ and two different advancing contact angles, $\varphi_A=90°$ and $\varphi_A=70°$

$$\varphi_R=45°<\varphi_1=70°,\ \varphi_2=53°<\varphi_A=70°$$

This means that the values of contact angles are adjusted between φ_A and φ_R so that the net force in the vertical direction is zero.

As a bubble radius is increased or contact angle hysteresis ($\varphi_A-\varphi_R$) is reduced, the bubble begins to slide along the vertical surface due to the dominance of buoyancy over the surface tension force. Figure 3 shows the effect of bubble radius on bubble motion for $\varphi_A=\varphi_R=45°$. Under this condition, the contribution of the surface tension

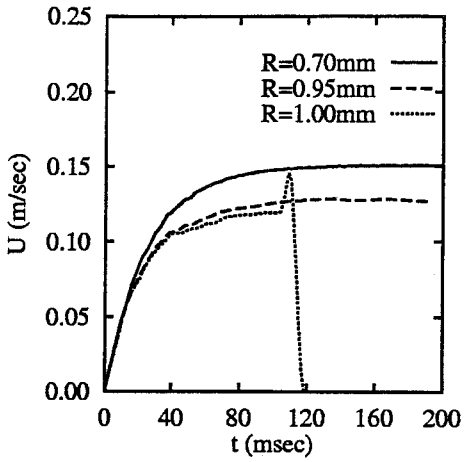

(a)

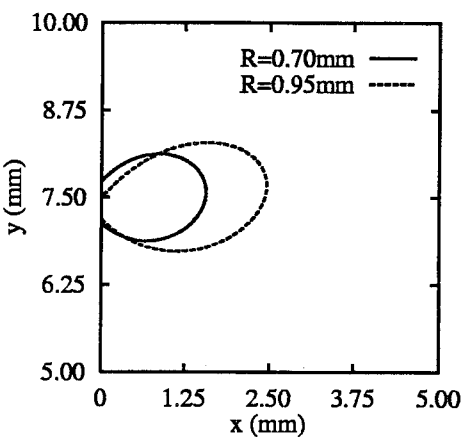

(b)

Fig. 3 Effect of bubble radius on bubble motion for $\varphi_A=\varphi_R=45°$: (a) bubble slide velocity and (b) bubble shape at a steady state

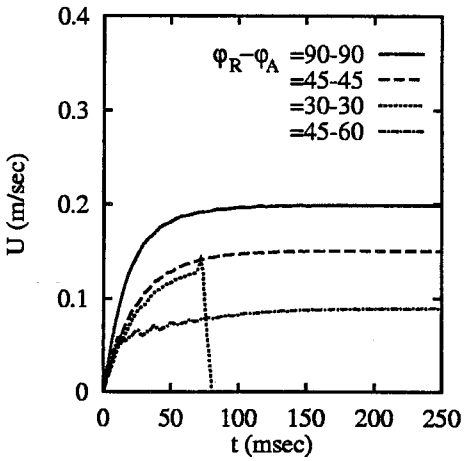

(a)

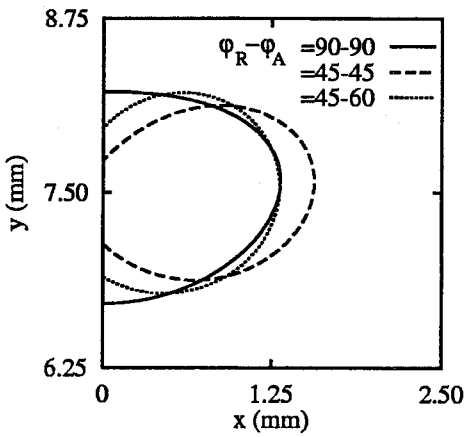

(b)

Fig. 4 Effect of contact angle on bubble motion without phase change: (a) bubble slide velocity and (b) bubble shape at a steady state with $R=0.7$ mm

to the net force in the vertical direction is zero. It is seen from Fig. 3 (a) that the slide velocity of a bubble initially increases with time and then attains a steady state when the buoyancy is balanced with the drag force caused by the liquid layer. As the bubble radius increases, the bubble shape at the steady state becomes oblate ellipsoidal rather than spherical due to the increase in the liquid drag force as shown in Fig. 3 (b). This in turn reduces the base area of the bubble in contact with the wall. As the bubble radius further increases up to 1 mm, the bubble detaches from the wall. The bubble just departing from the wall has quite a high slide velocity due to the loss of surface tension force and the friction force which tend to hold the bubble on the wall. However, as the bubble is injected into the relatively stationary liquid bulk, the bubble slide or rise velocity drops quickly with the increase in liquid drag. This behavior of bubble motion results in the peak at the slide velocity curve for $R=1$ mm as seen in Fig. 3 (a).

The dependence of bubble motion on contact angle is plotted in Fig. 4. It is seen that as the contact angle decreases the bubble slide velocity

decreases because the bubble shape with smaller contact angle induces more resistance from the liquid layer. Also, for a surface with contact angle hysteresis where the surface tension has a net force in the downward direction, the bubble slide velocity is observed to be reduced significantly.

3.2 A sliding bubble with phase change

Including the effect of phase change at the liquid-vapor interface, numerical simulations of a sliding bubble were performed. Mesh points of 98 $\times$194 were used and the computational domain was taken to be $3L\times6L$. Since nucleate boiling process is a cyclic process, conditions at the beginning of the cycle can only be determined if computation is carried out for a period that lasts more than one cycle. In this first study on a sliding bubble during nucleate boiling the cyclic simulation has not been done so far. Hence analysis was carried out by assuming that initially a linear temperature profile existed in the thermal boundary layer the thickness of which was evaluated from the correlation for the turbulent natural convective heat transfer on an isothermal vertical surface (Kays and Crawford, 1980).

Figure 5 shows the flow and temperature fields associated with the bubble growth and detachment for $\Delta T=1K$ and $\varphi_A=\varphi_R=45°$. During the early period of bubble growth, the bubble shape is almost spherical due to the effect of surface tension and the base area of the bubble in contact with the wall increases with time. However, as the drag force acting on the bubble increases with bubble growth, the bubble shape is deformed to be oblate ellipsoidal and the bubble base shrinks. When the bubble base area decreases up to zero, the bubble detaches from the wall. The bubble detached from the wall is injected into the liquid bulk rapidly due to the loss of surface tension force which holds the bubble on the wall. It is also observed from Fig. 5 that the isotherms initially parallel with the vertical surface are distorted as the bubble grows and slides. The isotherms are much more closely packed around the upper portion of the bubble than around the lower portion of the bubble due to the clockwise vortex near the bubble surface.

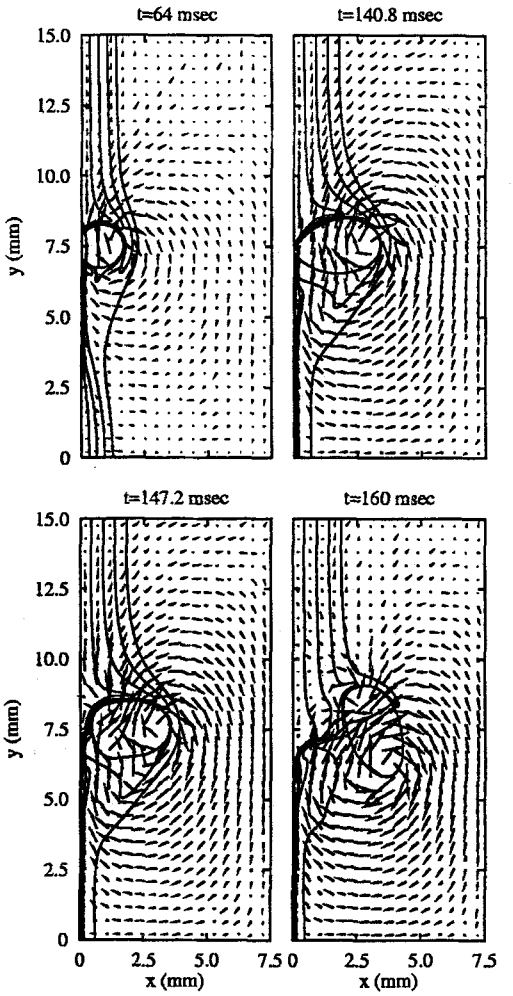

Fig. 5 Flow and temperature fields associated with the bubble growth and detachment for $\Delta T=1K$ and $\varphi_A=\varphi_R=45°$

Compared with the thermal boundary layer upstream of the bubble, the thermal boundary layer downstream is much thinner, which indicates the sliding bubble enhances the heat transfer significantly.

After the bubble detachment, the thermal boundary layers upstream and downstream of the bubble meet in the area vacated by the detaching bubble and then the thickness of the thermal boundary layer downstream increases with time.

The dependence of bubble growth and detachment on contact angle is plotted in Fig. 6. It is seen that as the contact angle increases, the bubble growth rate decreases. This is caused by the

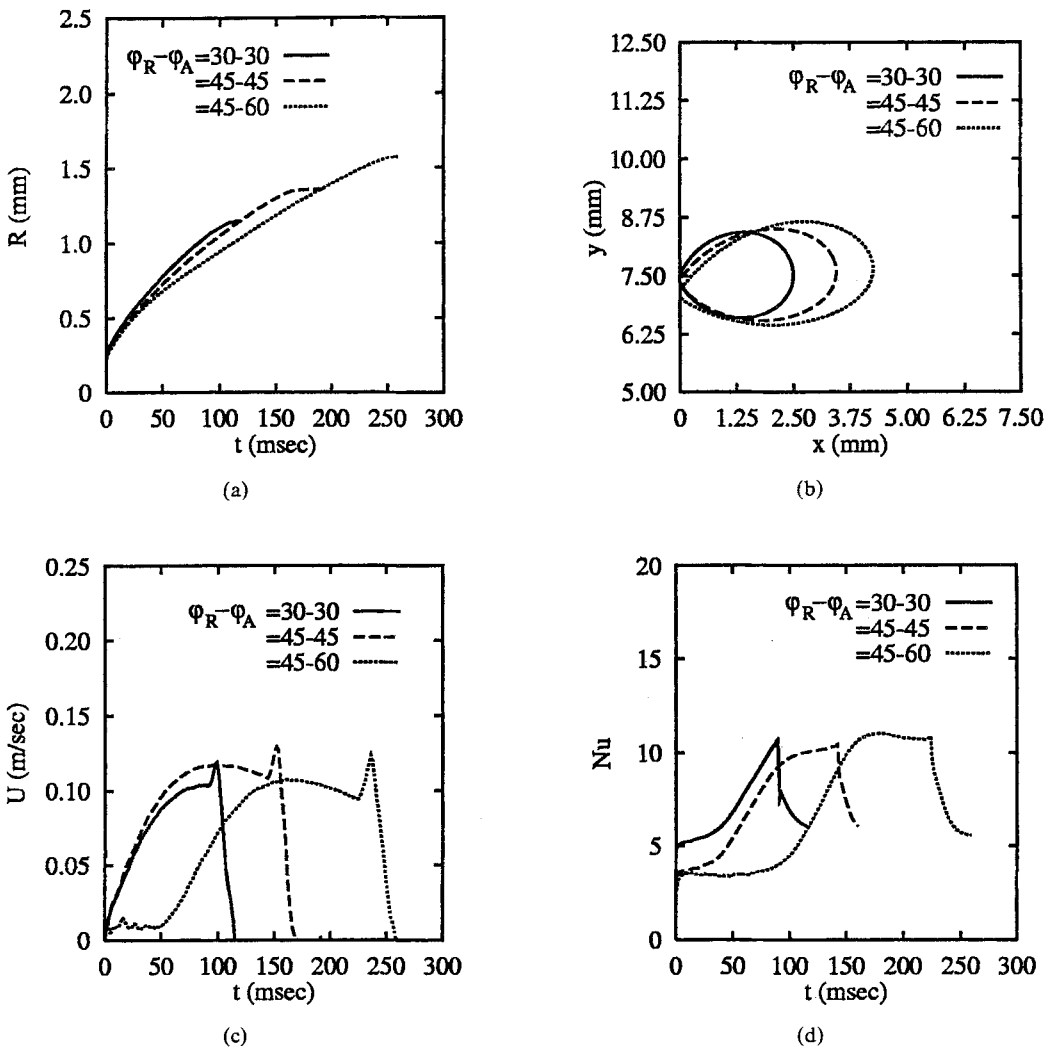

Fig. 6 Effect of contact angles on bubble motion for : $\Delta T=1K$ (a) bubble growth, (b) bubble shape at detachment, (c) bubble slide velocity and (d) Nusselt number

fact that the heat flux from the microlayer decreases with increase in the contact angle as expected by Eq. (6). Also, the bubble growth period and the bubble radius at detachment are observed to be larger as the contact angle increases. This indicates that the vapor volume required for bubble detachment increases as the contribution of surface tension increases with the contact angle. It is seen from Fig. 6 (c) and (d) that as the bubble slide velocity increases with time the Nusselt number based on the heat transfer coefficient averaged over the wall surface increases significantly. For $\varphi_A=\varphi_R=45°$ and $\Delta T=1K$, the maximum value of Nusselt number reaches up to 10.4, which is seven times larger than that obtained from the correlation for the turbulent natural convection. Also, it is noted that with contact angle hysteresis ($\varphi_R=45°$ and $\varphi_A=60°$) the bubble is nearly stationary during the early period of bubble growth, which is due to the net surface tension force in the downward direction. While the bubble is stationary, the Nusselt number is nearly constant. As the bubble grows and then the bubble begins to slide, the heat transfer increases. This indicates that the bubble slide velocity is a very important factor of

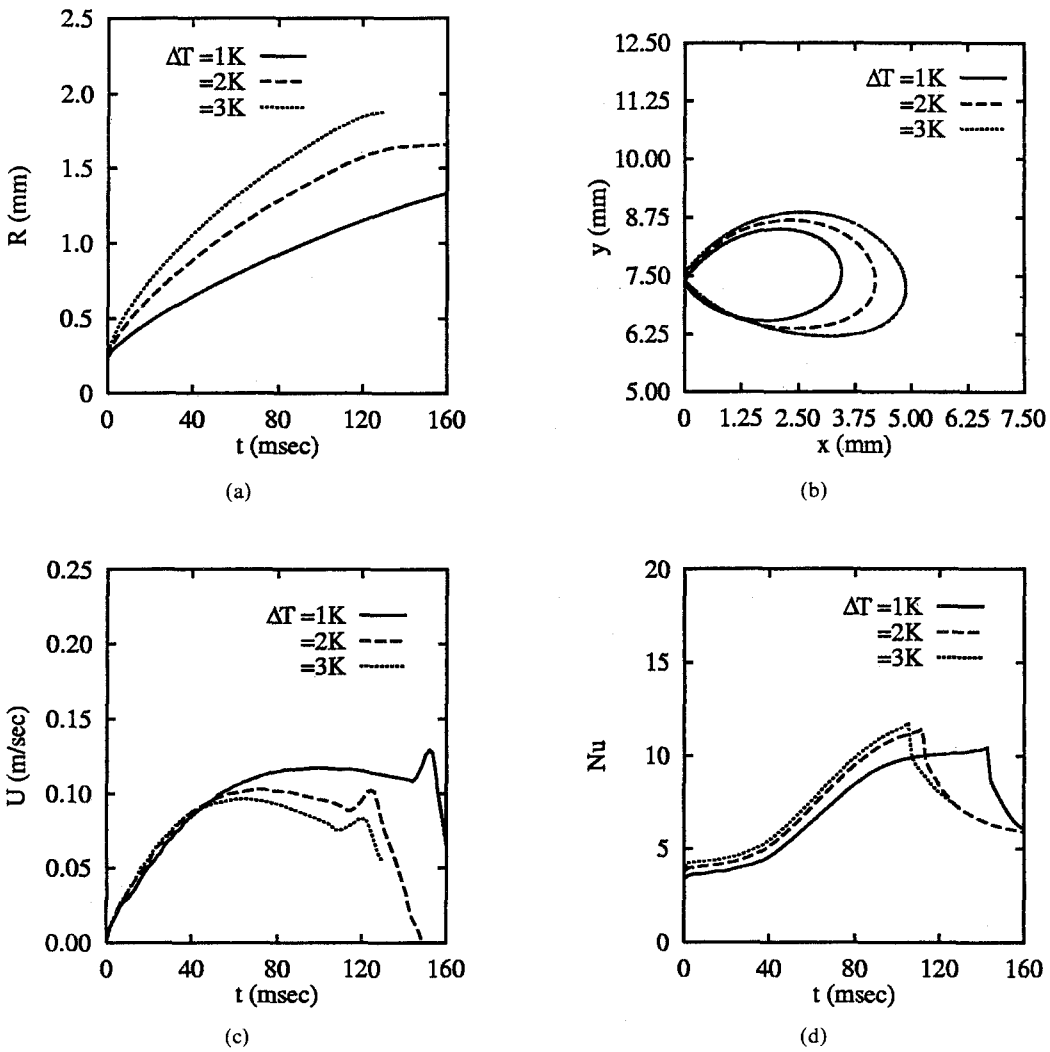

Fig. 7 Effect of wall superheat on bubble motion for $\varphi_A=\varphi_R=45°$: (a) bubble growth, (b) bubble shape at detachment, (c) bubble slide velocity and (d) Nusselt number

heat transfer enhancement during nucleate boiling.

Figure 7 shows the effect of wall superheat on the bubble motion. As the wall superheat increases, the bubble growth rate increases and the growth period decreases. Also, the bubble diameter at detachment increases with wall superheat. This means that for a fixed contact angle the bubble diameter at departure depends on the growth rate. It is seen from Fig. 7 (d) that as the wall superheat increases the Nusselt number increases slightly. This observation is different from the experimental observation reported in the literature. This is caused by the fact the present computations do not include the effect of the number of active sites which strongly depends on the wall superheat. This effect will be included in the future work.

4. Conclusions

In this study, the level set method was modified to include the effects of phase change at the interface and contact angle at the wall as well as to achieve mass conservation during the whole calculation procedure. Also, a simplified model to

predict the heat flux in a thin liquid microlayer was developed. The method was applied for simulation of a sliding bubble on a vertical surface. The numerical simulations demonstrated the bubble slide, growth and detachment process. Also, the flow and temperature fields influenced by the bubble motion were illustrated. Compared with heat transfer rate obtained from the correlation for the turbulent natural convection, the heat transfer associated with bubble growth and slide is observed to be enhanced significantly. Based on the computed results, the detaching bubble is found to be larger with the increase in contact angle and wall superheat.

Acknowledgement

The author would like to acknowledge the support from the Korea Research Foundation under Grant No. KRF-2000-003-E00005.

References

Kays, W. M. and Crawford, M. E., 1980, *Convective Heat and Mass Transfer*, McGraw-Hill Book Company, New York.

Khrustalev, D. and Faghri, A., 1995, "Heat Transfer During Evaporation on Capillary-Grooved Structures of Heat Pipes," *J. Heat Transfer*, Vol. 117, pp. 740~747.

Lay, J. H., and Dhir, V. K., 1995, "Shape of a Vapor Stem During Nucleate Boiling of Saturated Liquids," *J. Heat Transfer*, Vol. 117, pp. 394~401.

Lee, R. C., and Nydahl, J. E., 1989, "Numerical Calculation of Bubble Growth in Nucleate Boiling From Inception Through Departure," *J. Heat Transfer*, Vol. 111, pp. 474~479.

Marmur, A., 1998, "Contact-Angle Hysteresis on Heterogeneous Smooth Surfaces: Theoretical Comparison of the Captive Bubble and Drop Methods," *Colloids and Surfaces*, Vol. 136, pp. 209~215.

Ryskin, G. and Leal, L. G., 1984, "Numerical Simulation of Free-Boundary Problems in Fluid Mechanics. Part 2," *J. Fluid Mech.*, Vol. 148, pp. 19~35.

Son, G., Dhir, V. K., and Ramanujapu, N., 1999, "Dynamics and Heat Transfer Associated with a Single Bubble During Nucleate Boiling on a Horizontal Surface," *J. Heat Transfer*, Vol. 121, pp. 623~631.

Son, G. and Lee, S. R., 1999, "Numerical Simulation on Rising Bubble Behaviors in Water," Trans. *KSME*, Vol. 23, No. 12, pp. 1606~1613. (in Korean)

Sussman, M., Smereka, P., and Osher, S., 1994, "A Level Set Approach for Computing Solutions to Incompressible Two-Phase Flow," *J. Comput. Phys.*, Vol. 114, pp. 146~159.

Takata, Y., Shirakawa, H., Kuroki, T., and Ito, T., 1998, "Numerical Analysis of Single Bubble Departure from a Heated Surface," *Proc. 11th IHTC, Vol.* 4, pp. 355~360, Kyongju, Korea.

Thorncroft, G. E., Klausner, J. F., and Mei, R., 1998, "An Experimental Investigation of Bubble Growth and Detachment in Vertical Upflow and Downflow Boiling," *Int. J. Heat Mass Transfer*, Vol. 114, pp. 146~159.

Van Helden, W. G. J., Vander Geld, C. W. M., and Boot, P. G. M., 1995, "Forces on Bubbles Growing and Detaching in Flow Along a Vertical Wall," *Int. J. Heat Mass Transfer*, Vol. 38, pp. 2075~2088.

Wayner, P. C. Jr., 1992, "Evaporation and Stress in the Contact Line Region," *Proc. of The Engineering Foundation Conference On Pool and External Flow Boiling*, pp. 251~256, Santa Barbara, California.

Welch, S. W. J., 1998, "Direct Simulation of Vapor Bubble Growth," *Int. J. Heat Mass Transfer*, Vol. 41, pp. 1655~1666.